Pathol. Oncol. Res. (2010) 16:541–545
DOI 10.1007/s12253-010-9260-z

Elevated Osteopontin Expression and Proliferative/Apoptotic Ratio in the Colorectal Adenoma–Dysplasia–Carcinoma Sequence

Gábor Valcz · Ferenc Sipos · Tibor Krenács · Jeannette Molnár · Árpád V. Patai · Katalin Leiszter · Kinga Tóth · Norbert Solymosi · Orsolya Galamb · Béla Molnár · Zsolt Tulassay

Received: 2 December 2009 / Accepted: 10 March 2010 / Published online: 27 March 2010

Abstract Colorectal cancer progression is characterized by altered epithelial proliferation and apoptosis and by changed expression of tumor development regulators. Our aims were to determine the proliferative/apoptotic epithelial cell ratio (PAR) in the adenoma–dysplasia–carcinoma sequence (ADCS), and to examine its association with osteopontin (OPN), a previously identified protein product related to cancer development. One mm diameter cores from 13 healthy colons, 13 adenomas and 13 colon carcinoma samples were included into a tissue microarray (TMA) block. TUNEL reaction and Ki-67 immunohistochemistry were applied to determine the PAR. The osteopontin protein was also immunodetected. Stained slides were semiquantitatively evaluated using digital microscope and statistically analyzed with logistic regression and Fisher's exact test. The PAR continuously increased along the ADCS. It was significantly ($p<0.001$) higher in cancer epithelium (8.84±7.01) than in adenomas (1.40±0.78) and in normal controls (0.89±0.21) ($p<0.001$). Also, significant positive correlation was observed between elevated PAR and the expression of osteopontin. Cytoplasmic OPN expression was weak in healthy samples. In contrast, cytoplasmic immunoreaction was moderately intensive in adenomas, while in colon cancer strong, diffuse cytoplasmic immune staining was detected. Increasing PAR and OPN expression along ADCS may help monitoring colorectal cancer progression. The significantly elevated OPN protein levels we found during normal epithelium to carcinoma progression may contribute to the increased fibroblast–myofibroblast transition determining stem cell niche in colorectal cancer.

Keywords Proliferative/apoptotic ratio · Adenoma–dysplasia–carcinoma sequence · Gene expression · Tissue microarray

G. Valcz (✉) · F. Sipos · Á. V. Patai · K. Leiszter · K. Tóth · N. Solymosi · O. Galamb · B. Molnár · Z. Tulassay
2nd Department of Internal Medicine, Semmelweis University,
Cell Analysis Laboratory,
Szentkirályi Street 46,
1088 Budapest, Hungary
e-mail: valczg@yahoo.com

O. Galamb · B. Molnár · Z. Tulassay
Molecular Medicine Research Group,
Hungarian Academy of Sciences,
Budapest, Hungary

T. Krenács
1st Department of Pathology and Experimental Oncology,
Semmelweis University,
Budapest, Hungary

J. Molnár
National Institute of Food and Nutrition Science,
Budapest, Hungary

Introduction

The synchronization of cell functions like cell growth, proliferation, and migration is mediated via signal transduction pathways both in healthy tissues and in tumors. These processes are influenced by several biochemical systems, such as adhesion molecules, chemotactic and growth factors [1]. Several among these regulatory ligands play a role in the information flow between local stem cells and their specific microenvironment called "niche" [2]. The quantitative and qualitative changes of secreted regulators by niche cells may cause alterations in stem cell activation and influence the rate of epithelial cells in the proliferative and apoptotic phase.

This process is linked to the appearance of dysplastic epithelium and adenoma development. The next step is represented by the malignant transformation of dysplastic epithelium and finally carcinoma formation. The whole process is called adenoma–dysplasia–carcinoma sequence (ADCS), which is the most frequent way of colorectal cancer (CRC) development [3–5].

The mathematical transformation of the altered stem cell activation is manifested by a shift in the relative ratio of proliferative and apoptotic epithelial cells (proliferative/apoptotic ratio, PAR). One possible way of quantifying the change in the PAR is the detection of growth faction of tumor using anti-Ki-67 protein immunostaining [6] and visualization of nuclear chromatin fragmentation (as a hallmark of apoptosis) applying the TUNEL (*T*erminal deoxynucleotidyl transferase-mediated d*U*TP *N*ick *E*nd-*L*abeling) method [7].

In our study we payed specific attention to the changes of osteopontin (OPN, SPP1) expression due to its multiple biological functions [8] and because of the significant changes in mRNA levels during tumor development that we had detected in our previous studies [9]. Osteopontin is a sialic acid- and aspartate-rich chemokine-like glycoprotein [10, 11], which has a role in metastasis development [11], cell adhesion [12], angiogenesis [13, 14] and apoptosis inhibition [14, 15]. The roles of OPN in cell proliferation are multiple and paradox. Huang et al (2004) described that it inhibits proliferation of MC3T3-E1 pre-osteoblastic cells in vitro [16], while others reported a opposite effect on other cell types [17, 18]. Osteopontin may have a potential role in malignant transformation via connection to CD44 or/and integrin (αvβ1, αvβ3, αvβ5, α4β1, α5β1, α8β1 and α9β1) receptors [19]. This interaction initiates connection phosphorylation and activativation several kinases (e.g. phosphoinositide 3-kinase, NIK, PLC, PKC, MAPK) which transactivate various transcription factors, including NFkB and AP-1. These processes may play a fundamental role in malignant transformation [11]. OPN is essential in fibroblast to myofibroblast and epithelial to mesenchymal transition (EMT) [20, 21]. Osteopontin does not induce myofibroblast differentiation *per se* [20], but exogenous OPN facilitates the adhesion of mouse ocular fibroblast *in vitro* [22]. Furthermore, although TGF-β is the main regulator of fibroblast to myofibroblast transition, it does not induce conversion in OPN null mice [20]. By modifying the fibroblast/myofibroblast ratio, OPN may play a role by affecting the niche cell composition during both inflammation and carcinogenesis.

In this study, we examined the correlation between the epithelial proliferative/apoptotic ratio in relation to the expression of the osteopontin protein, the mRNA of which we found significantly elevated during the adenoma–dysplasia–carcinoma sequence [9].

Materials and Methods

Surgically removed tissue samples from 13 colon adenomas, 13 colon cancers and 13 adjacent healthy colon samples were fixed in formalin and embedded in paraffin. Core biopsies with 1 mm diameter were cut and placed into a recipient block, from which 4 μm-thick tissue microarray (TMA) slides were prepared. TMA slides were deparaffinated and rehydrated.

TUNEL Method

After 20 min digestion with 20 μg/ml proteinase-K, 50 μl TUNEL (TUNEL In Situ Cell Death Detection Kit, Fluorescein, Roche, 11684795910) reaction mixture was added to the TMA slides (5 μl TdT enzyme + 45 μl dUTP). Then the samples were incubated in a dark humidified chamber at 37°C for 120 min.

Proliferation

After TUNEL reaction and antigen retrieval with TRIS-EDTA buffer (performed in a microwave oven at 900 W for 10 min and at 370 W for 40 min), non-specific blocking was achieved by using 1% bovine serum albumin. TMA slides were incubated with anti-Ki-67 (Clone: MIB-1, M7240, 1:100 dilution, Dako) monoclonal antibody for 60 min, and then were labeled with Alexa Fluor 546(F(ab') 2 (1:200 dilution, 30 min, Invitrogen).

Osteopontin Immunohistochemistry

Endogenous peroxidase blocking (0.5% hydrogen peroxide and methanol mixture, 30 min, room temperature) and antigen retrieval (Target Retrieval Solution, S1699, Dako, in pH 6 buffer, performed in a microwave oven at 900 W for 10 min and at 370 W for 40 min) were carried out on dewaxed TMA samples. Non-specific blocking with 1% bovine serum albumin was applied. Immunohistochemical detection of osteopontin was carried out in a humidified chamber using an anti-OPN polyclonal antibody (AB1870, 1:200 dilution, 60 min, Chemicon). EnVision + HRP system (Labeled Polymer Anti-Rabbit, K 4003, Dako) and diaminobenzidine - hydrogen peroxidase - chromogen - substrate system (Cytomation Liquid DAB + Substrate Chromogen System, K3468, Dako) were used for signal conversion. Finally, hematoxylin co-staining was carried out.

Slide digitalization

TMA slides stained with fluorescent labels were digitalized with a high resolution digital scanner (MIRAX Desk, Zeiss,

Gottingen), using high numeric aperture (0.8) ×20 objective lens and an AxioCam Mrm Rev.3 high resolution camera connected to the scanner. The size of the digital slides ranged between 500–1000 MB, and they were accessed through a computer monitor by using the Mirax Viewer software.

Evaluation, Statistical Analysis

Digital slides were examined with a digital microscope (MIRAX Viewer, Version:1.11.43.0). The exact cell counting was carried out on digital slides using a built-in software module called Marker Counter, which allowed us to estimate the relative ratio of different cells (proliferative, normal and apoptotic).

TUNEL and Ki-67 positivity were associated with strong nuclear labeling. Depending on the sample size, 800–1000 crypt epithelial cells were counted.

We have made the Ki-67/TUNEL ratio comparable to the different protein expression changes by setting up an empirical scale. The ratio–scale transformation was made on the basis of the following criteria: if the ratio was below 1, then the value was −2; if it was between 1 and 2, the value was 0; if it was between 2 and 5, the value was 1; and if it was over 5, the value was 2.

The score of osteopontin immunohistochemistry (bright-field, also digitalized) was 0 if weak, 1 if moderate, and 2 if strong cytoplasmic labeling was observed. Scores representing the intensity of the immunohistochemical reaction were evaluated using the TMA module software. For statistical evaluation, logistic regression and Fisher's exact tests were applied.

Results

The proliferative/apoptotic ratio continuously increased during the ADCS progression (Fig. 1). The number of apoptotic cells in the normal colonic epithelium barely surpassed the proliferative cell number. The PAR was 0.89± 0.21. Proliferative cells were predominantly localized in the basal crypt section, whereas apoptotic cells appeared in the higher parts of the crypt. In adenoma samples, the number of mitotic cells was higher (1.40±0.78)) and the ratio of apoptotic cells was moderately higher than the proportion of proliferative cells. A significantly ($p<0.001$) higher PAR was measured in the tumorous epithelium (8.84±7.01) than in adenomas or in normal colon samples (Fig. 2). A higher percentage of epithelial cells showed Ki-67 expression in tumor samples but we found only a few apoptotic epithelial cells.

Osteopontin expression correlated significantly with the proliferative/apoptotic ratio. It is important to note that OPN protein expression was limited to the cytoplasma, and we did not detect visible immunopositivity in the area of the nucleus. In normal samples, only weak, discrete, diffuse cytoplasmic osteopontin immunoreaction was found (Fig. 3 N). In adenomas, we detected a moderately intensive diffuse cytoplasmic immunoreaction (Fig. 3 AD), while in colon cancer we found strong, diffuse cytoplasmic immune staining (Fig. 3 CRC). Results are also visualized in an association plot (Fig. 4). In addition, some stromal and immune cells, predominantly macrophages and lymphocytes showed moderate OPN expression during colorectal carcinoma development.

Discussion

During tumor development, cell fractions undergoing proliferation, differentiation and apoptosis, differ significantly from those in normal tissue. In this study, we tested the potential association between the proliferative/apoptotic ratio and the expression of osteopontin, a protein supposed to contribute to cancer progression and which we earlier detected at mRNA level in colon cancer [9]. Here we show that the colorectal adenoma–dysplasia–carcinoma sequence can be characterized with a significantly elevated epithelial

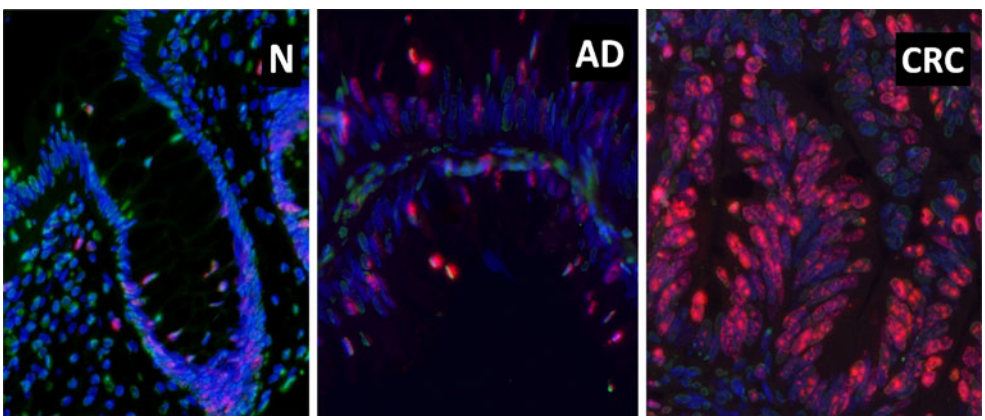

Fig. 1 Changes in the number of proliferative (red nuclei) and apoptotic (green nuclei) cells during the colorectal ADCS. Images were taken using a digital microscope: normal tissue (N), adenoma (AD) and carcinoma (CRC). The number of proliferative cells increases during the ADCS (30-fold magnification)

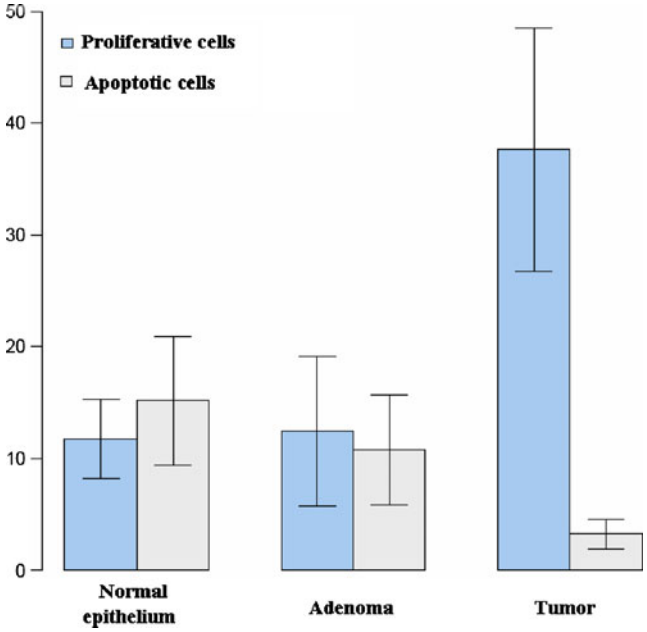

Fig. 2 Changes in the number of proliferative (blue column) and apoptotic (red column) cells during the colorectal ADCS. The number of proliferative cells is elevated in adenomas compared to normal colonic epithelium, and the increase is even more notable/significant in colon cancer

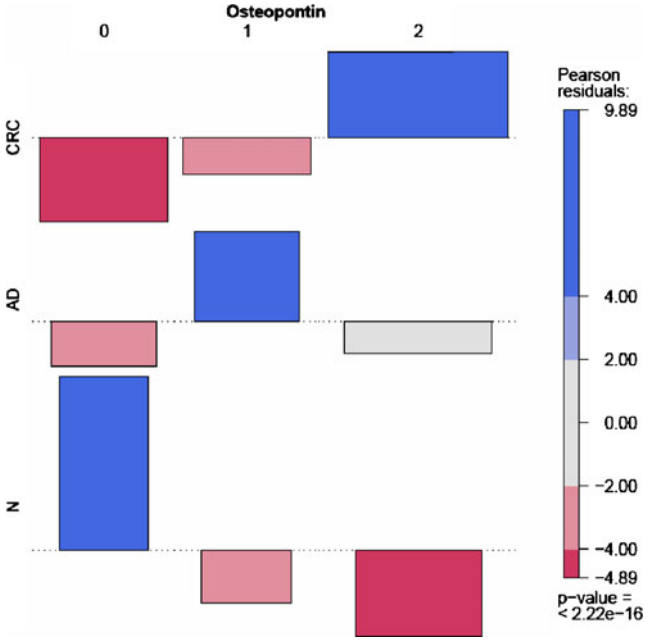

Fig. 4 Association plot of cytoplasmic expression level of osteopontin in the colonic epithelium: normal sample (N), adenoma (AD) and carcinoma (CRC). The differences (Pearson's residuals) between the observed and expected frequencies of contingency table are presented with rectangles. Height and width of *bars* are proportional to Pearson's residuals, and expected counts respectively. Sign of *bar* represents if observed count is higher or lower than it is expected

cell PAR and cytoplasmic expression of osteopontin protein in biopsy samples representing different stages of colorectal carcinogenesis. Although osteopontin was also described to interact with nuclear cell cycle regulators [23], we could not detect a significant amount of visible OPN in nuclear localization.

The role of OPN of epithelial origin as extra- and intracellular ligand has not been revealed at every detail. It may have an important functions in the fibroblast–myofibroblasts or fibroblast–epithelial cells transdifferentiation [20, 21]. Since in colorectal carcinoma the number of myofibroblasts showed a negative correlation with the number of inflammatory cells, the main sources of OPN [24] may need to originate also from other sources. According to our hypothesis, the OPN produced by significant amount by epithelial cells, appears in the stroma as a consequence of apoptosis, necrosis or active secretion and influences the number of myofibroblasts developing from fibroblasts or epithelial cells. Hawinkels et al. (2009) reported that the number of myofibroblasts show a positive correlation with stromal TGF-β during the normal–adenoma–carcinoma sequence [25]. Elevated expression of these two main regulators may play a role in the development of an abnormal microenvironment

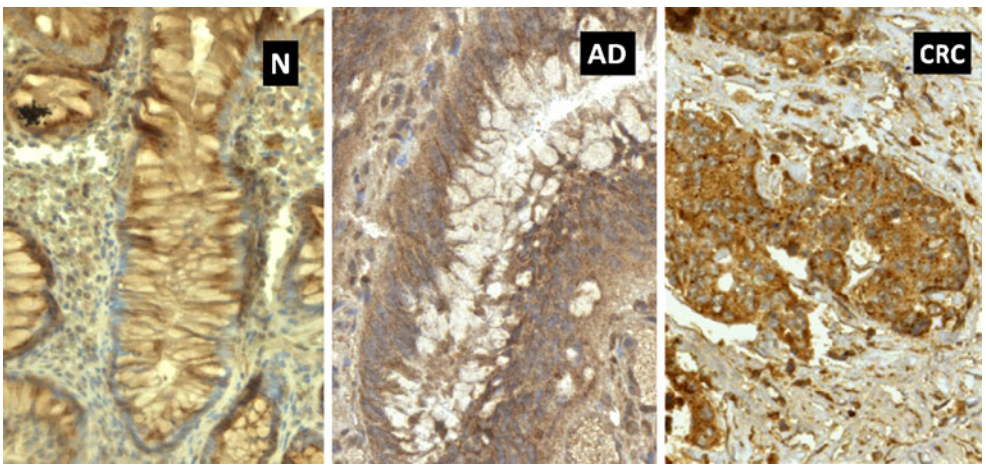

Fig. 3 Changes of osteopontin expression during the colorectal ADCS: normal colonic epithelium (N), adenoma (AD) and colon cancer (CRC) (35-fold magnification). The epithelial intensity of osteopontin immunoreaction increases during the ADCS

which may affect epithelial proliferation and malignant transformation by altered stem cell activation.

Potential methods of osteopontin inhibition can have promising potential in cancer therapy. One option is the inhibition of the OPN protein by various antibodies [26]. The inhibition of OPN may lead to the suppression of cell adhesion [12], tumor growth and metastasis formation [27, 28] in several types of cancer. The multiple and complex roles of OPN in tumor development are not yet fully elucidated and require further investigation in the future. Based on the results of this study and on previously published data, we hope that OPN becomes a molecular diagnostic marker and a potential target of therapy in the treatment of various cancers.

In summary, our results suggest that elevating PAR and OPN expression along the ADCS can assist in monitoring the progression of colorectal cancer.

Acknowledgements We thank Gabriella Kónya (Cell Analysis Laboratory, 2nd Department of Medicine, Semmelweis University, Budapest, Hungary) for her help in performing this study. This study was supported by the National Office for Research and Technology, Hungary (TECH_08-A1/2-2008-0114 grant).

References

1. Burgess AW (1998) Growth control mechanisms in normal and transformed intestinal cells. Philos Trans R Soc Lond B Biol Sci 353:903–909
2. Walker MR, Patel KK, Stappenbeck TS (2009) The stem cell niche. J Pathol 217:169–180
3. Fearon ER, Vogelstein B (1990) A genetic model for colorectal tumorigenesis. Cell 61:759–767
4. Vogelstein B, Fearon ER, Hamilton SR et al (1988) Genetic alterations during colorectal-tumor development. N Engl J Med 319:525–532
5. Leslie A, Carey FA, Pratt NR et al (2002) The colorectal adenoma–carcinoma sequence. Br J Surg 89:845–860
6. Scholzen T, Gerdes J (2000) The Ki-67 protein: from the known and the unknown. J Cell Physiol 182:311–322
7. Sipos F, Zágoni T, Molnár B et al (2002) Changes in the proliferation and apoptosis of colonic epithelial cells in correlation with histologic activity of ulcerative colitis. Orv Hetil 143:2485–2488
8. Tuck AB, Chambers AF (2001) The role of osteopontin in breast cancer: clinical and experimental studies. J Mammary Gland Biol Neoplasia 6:419–429
9. Galamb O, Sipos F, Spisák S et al (2009) Potential biomarkers of colorectal adenoma–dysplasia–carcinoma progression: mRNA expression profiling and in situ protein detection on TMAs reveal 15 sequentially upregulated and 2 downregulated genes. Cell Oncol 31:19–29
10. Wai PY, Kuo PC (2008) Osteopontin: regulation in tumor metastasis. Cancer Metastasis Rev 27:103–118
11. Rangaswami H, Bulbule A, Kundu GC (2006) Osteopontin: role in cell signaling and cancer progression. Trends Cell Biol 16:79–87
12. Bautista DS et al (1994) Inhibition of Arg-Gly-Asp (RGD)-mediated cell adhesion to osteopontin by a monoclonal antibody against osteopontin. J Biol Chem 269:23280–23285
13. Hirama M, Takahashi F, Takahashi K et al (2003) Osteopontin overproduced by tumor cells acts as a potent angiogenic factor contributing to tumor growth. Cancer Lett 198:107–117
14. Weber GF (2008) Molecular mechanisms of metastasis. Cancer Lett 270:181–190
15. Lin YH, Yang-Yen HF (2001) The osteopontin-CD44 survival signal involves activation of the phosphatidylinositol 3-kinase/Akt signaling pathway. J Biol Chem 276:46024–46030
16. Huang W, Carlsen B, Rudkin G et al (2004) Osteopontin is a negative regular of proliferation and differentiation in MC3T3-E1 pre-osteoblastic cells. Bone 34:799–808
17. Panda D, Kundu GC, Lee BI et al (1997) Potential roles of osteopontin and alphaVbeta3 integrin in the development of coronary artery restenosis after angioplasty. Proc Natl Acad Sci USA 94:9308–9313
18. Elgavish A, Prince C, Chang PL (1998) Osteopontin stimulates a subpopulation of quiescent human prostate epithelial cells with high proliferative potential to divide in vitro. Prostate 35:83–94
19. El-Tanani MK, Campbell FC, Kurisetty V et al (2006) The regulation and role of osteopontin in malignant transformation and cancer. Cytokine Growth Factor Rev 17:463–474
20. Lenga Y, Koh A, Perera AS et al (2008) Osteopontin expression is required for myofibroblast differentiation. Circ Res 102:319–327
21. Saika S, Shirai K, Yamanaka O et al (2007) Loss of osteopontin perturbs the epithelial–mesenchymal transition in an injured mouse lens epithelium. Lab Invest 87:130–138
22. Miyazaki K, Okada Y, Yamanaka O et al (2008) Corneal wound healing in an osteopontin-deficient mouse. Invest Ophthalmol Vis Sci 49:1367–1375
23. Junaid A, Moon MC, Harding GE et al (2007) Osteopontin localizes to the nucleus of 293 cells and associates with polo-like kinase-1. Am J Physiol Cell Physiol 292:919–926
24. Katenkamp D, Berndt R, Perevoshchikov A et al (1984) Ultrastructural observations of the stroma of human colon carcinomas with special regard to myofibroblasts. Arch Geschwulstforsch 54:301–308
25. Hawinkels LJ, Verspaget HW, van der Reijden JJ et al (2009) Active TGF-beta1 correlates with myofibroblasts and malignancy in the colorectal adenoma–carcinoma sequence. Cancer Sci 100:663–670
26. Weber GF (2001) The metastasis gene osteopontin: a candidate target for cancer therapy. Biochim Biophys Acta 1552:61–85
27. Dai J, Li B, Shi J et al (2010) A humanized anti-osteopontin antibody inhibits breast cancer growth and metastasis in vivo. Cancer Immunol Immunother 59:355–366
28. Thalmann GN, Sikes RA, Devoll RE et al (1999) Osteopontin: possible role in prostate cancer progression. Clin Cancer Res 5:2271–2277